



This is a repository copy of *Modelling of non-minimum phase effects in discrete-time norm optimal iterative learning control*.

White Rose Research Online URL for this paper:
<http://eprints.whiterose.ac.uk/74694/>

Monograph:

Owens, D.H. and Chu, B. (2009) Modelling of non-minimum phase effects in discrete-time norm optimal iterative learning control. Research Report. ACSE Research Report no. 1005 . Automatic Control and Systems Engineering, University of Sheffield

Reuse

Unless indicated otherwise, fulltext items are protected by copyright with all rights reserved. The copyright exception in section 29 of the Copyright, Designs and Patents Act 1988 allows the making of a single copy solely for the purpose of non-commercial research or private study within the limits of fair dealing. The publisher or other rights-holder may allow further reproduction and re-use of this version - refer to the White Rose Research Online record for this item. Where records identify the publisher as the copyright holder, users can verify any specific terms of use on the publisher's website.

Takedown

If you consider content in White Rose Research Online to be in breach of UK law, please notify us by emailing eprints@whiterose.ac.uk including the URL of the record and the reason for the withdrawal request.

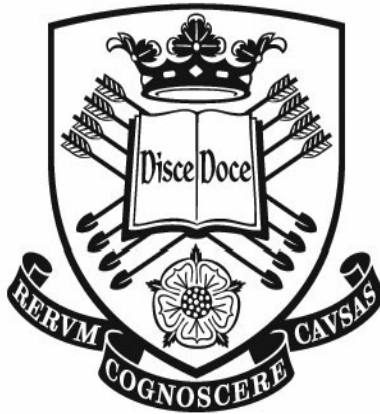


eprints@whiterose.ac.uk
<https://eprints.whiterose.ac.uk/>

Modelling of Non-minimum Phase Effects in Discrete-time Norm Optimal Iterative Learning Control

David H Owens, Bing Chu

Department of Automatic Control and Systems Engineering,
University of Sheffield,
Mappin Street, Sheffield, S1 3JD, UK



Research Report No. 1005

Department of Automatic Control and Systems Engineering
The University of Sheffield
Mappin Street, Sheffield,
S1 3JD, UK

October 2009

Modelling of non-minimum phase effects in discrete-time norm optimal iterative learning control

David H Owens, Bing Chu ^a

^a*Department of Automatic Control and Systems Engineering
The University of Sheffield, Mappin Street, Sheffield S1 3JD, UK*

Abstract

The subject of this paper is the modelling of the influence of non-minimum phase discrete-time system dynamics on the performance of norm optimal iterative learning control (NOILC) algorithms with the intent of explaining the observed phenomenon and predicting its primary characteristics. It is established that performance in the presence of non-minimum phase plant zeros typically has two phases. These consist of an initial fast monotonic reduction of the L_2 error norm (mean square error) followed by a very slow asymptotic convergence. Although the norm of the tracking error does eventually converge to zero, the practical implications over a finite number of trials is apparent convergence to a non-zero error. The source of this slow convergence is identified using the singular value distribution of the system's all pass component. A predictive model of the onset of slow convergence behavior is developed as a set of linear constraints and shown to be valid when the iteration time interval is sufficiently long. The results provide a good prediction of the magnitude of error norm where slow convergence begins. Formulae for this norm and associated error time series are obtained for single-input single-output systems with several non-minimum phase zeros outside the unit circle using Lagrangian techniques. Numerical simulations are given to confirm the validity of the analysis.

Key words: iterative learning control; non-minimum phase systems; singular value decomposition; all pass systems

1 Introduction

Iterative learning control (ILC) is a control method for improving tracking performance of systems that execute the same task repeatedly by learning from past actions. Applications of ILC can be widely found in areas including industrial robot manipulators [1], [2], chemical batch processes [3], [4], some medical applications [?] and manufacturing [5], [6]. Since the original work [7] in the mid 1980s, the general area of ILC has been the subject of substantial research effort. An initial source for the literature here are the survey papers [8], [9] and [10].

In principle, ILC has shown its capability of attaining high tracking performance. However, as in all control algorithms, including the familiar feedback control paradigm, there are limitations to what ILC can achieve depending on the characteristics of the plant. In particular, when dealing with non-minimum phase systems, ILC algorithms will be seen to result in a fast reduction in the tracking error initially and then slow convergence

thereafter, which is undesirable in practice. The existence of the problem was originally realized in [11] and several methods [12], [13], [14] have been proposed to solve this problem. It is believed, however, that the basis of the slow convergence phenomenon is not fully understood and new design methods to solve this problem are still needed.

In this paper, the performance of norm-optimal iterative learning control (NOILC) algorithms for the discrete time linear time invariant non-minimum phase systems is studied in terms of the singular value structure associated with an all-pass network arising from the plant transfer function. The paper is organized as follows. In Section 2 the problems observed when NOILC is applied to non-minimum phase systems is introduced briefly with emphasis on illustrating the primary observed characteristics. An ability to predict this behaviour and compute its effect in a given case is the focus for the following discussion. In Section 3, some fundamental results for matrix representation of all pass system are reviewed and the basis of the slow convergence of NOILC algorithms applied to non-minimum phase systems is identified in terms of an subspace decomposition of the output (time series) space. Each component is seen to

* Corresponding author David H Owens. Email: D.H.Owens@sheffield.ac.uk.

be associated with a subspace in which the NOILC algorithm exhibits different convergence properties. This is used in Section 4 to motivate and construct an approximate model for the slow convergence in terms of a modified NOILC problem with additional linear inner product constraints. This model is then used to predict the transient and asymptotic performance of the algorithm and identify/predict important features of the convergence. Numerical simulations are presented in Section 5 to verify the analysis results and finally, conclusions are given in Section 6.

2 Problem Formulation

In this section, system modelling is summarised and the ILC problem is formulated. The slow convergence observed when NOILC is applied to non-minimum phase plants is then illustrated by a simulation example.

2.1 ILC: Matrix Modelling of Plant dynamics

Consider the following discrete time, single-input single-output, linear time-invariant system with transfer function $G(z) = C(zI - A)^{-1}B + D$ and state space model

$$\begin{aligned} x_k(t+1) &= Ax_k(t) + Bu_k(t) \\ y_k(t) &= Cx_k(t) + Du(t), \quad t = 0, 1, 2, \dots, N \end{aligned} \quad (1)$$

where t is the time index (i.e. sample number), k is the iteration number and $u_k(t)$, $x_k(t)$, $y_k(t)$ are input, state and output of the system at time t on iteration k . The initial condition $x_k(0) = x_0$, $k = 1, 2, \dots$ is the same for all iterations. The control objective is to track a given reference signal $r(t)$ defined on a finite duration $t \in [0, N]$ (i.e. t is the sample number for time series of length $N+1$) and to do so by repeated execution of the task and data transfer from task to task. Mathematically, following the final time $t = N$, the state is reset to x_0 and time is reset to $t = 0$, a new iteration is started and, again, the system is required to track the same reference.

Remark 1 *In the literature, iterations are variously termed iterations, trials, repetitions and passes. There is, as yet, no agreement on common terminology.*

Before presenting the main results, the matrix operator form of the dynamics is demonstrated using the well-known, so-called lifted-system representation, which provides a straightforward ' $N \times N$ matrix' approach in the analysis of discrete-time ILC [15], [16], [17].

Denote the relative degree (pole-zero excess) of the system by $k^* \geq 0$. Then system model (1) on the k^{th} iteration can be expressed in an equivalent form

$$y_k = Gu_k + d, \quad (2)$$

where the $(N+1-k^*) \times 1$ vectors of input, output and reference time series u_k, y_k, r (resp.) are defined as

$$\begin{aligned} u_k &= \begin{bmatrix} u_k(0) & u_k(1) & \dots & u_k(N-k^*) \end{bmatrix}^T \\ y_k &= \begin{bmatrix} y_k(k^*) & y_k(2) & \dots & y_k(N) \end{bmatrix}^T \\ r &= \begin{bmatrix} r(k^*) & r(2) & \dots & r(N) \end{bmatrix}^T \end{aligned} \quad (3)$$

with tracking error vector $e = r - y$. Also

$$d = \begin{bmatrix} CA^{k^*}x_0, CA^{k^*+1}x_0, \dots, CA^N x_0 \end{bmatrix}^T \quad (4)$$

and G is defined by the $(N+1-k^*) \times (N+1-k^*)$ matrix when $k^* = 0$

$$G = \begin{bmatrix} D & 0 & 0 & \dots & 0 & 0 \\ CB & D & 0 & \dots & 0 & 0 \\ CAB & CB & D & 0 & \ddots & 0 \\ CA^2B & CAB & \ddots & \ddots & 0 & \vdots \\ \vdots & \ddots & \ddots & CB & D & 0 \\ CA^{N-1}B & \dots & \dots & CAB & CB & D \end{bmatrix} \quad (5)$$

or, when $k^* \geq 1$,

$$G = \begin{bmatrix} CA^{k^*-1}B & 0 & \dots & 0 & 0 \\ CA^{k^*}B & CA^{k^*-1}B & \ddots & 0 & 0 \\ CA^{k^*+1}B & CA^{k^*}B & \ddots & \ddots & \vdots \\ \vdots & \ddots & \ddots & CA^{k^*-1}B & 0 \\ CA^{N-1}B & \dots & \dots & CA^{k^*}B & CA^{k^*-1}B \end{bmatrix}.$$

Remark 2 *By construction, the matrix G is nonsingular and hence the control times series u_∞ that produces the output $y = r$ can be computed formally as $u_\infty = G^{-1}(r - d)$. Hence, without loss of generality, it can be assumed that $d = 0$ by incorporating it into the reference signal (i.e. replacing r by $r - d$). In this case*

$$y_k = Gu_k \quad (6)$$

Remark 3 *The lifted representation matrix G , although derived from $G(z)$ operates on its time series vectors in a manner described by the transfer function $z^{k^*}G(z)$.*

The above representation changes the original ILC problem into a MIMO tracking problem [15], [16]. All the following discussions will be based on this representation

although note [17] that all calculations based on matrix descriptions can be undertaken as calculations using the underlying state space model or associated transfer function.

2.2 ILC: Problem Formulation

Tracking error improvements from iteration to iteration are achieved in ILC using the following general control updating law

$$u_{k+1} = f(e_{k+1}, \dots, e_{k-s}, u_k, \dots, u_{k-r}), \quad (7)$$

where $e_j = r - y_j$ is the tracking error time series vector on the j^{th} trial. When $s > 0$ or $r > 0$, (7) is called a high order updating law. This paper only considers algorithms of the form $u_{k+1} = f(e_k, u_k)$. For higher order algorithms, please refer to [18], [19] and the references therein.

The ILC Algorithm Design Problem: The ILC algorithm design problem can now be stated as finding a control updating law (7) such that the system output has the asymptotic property that $e_k \rightarrow 0$ as $k \rightarrow \infty$.

Remark 4 *In practice, this definition is extended to require that convergence to zero is rapid (hence reducing simulation and experimental time and costs) and ideally monotonic in the sense that the mean square tracking error reduces from trial to trial whenever possible.*

There are many design methods to solve the ILC problem. The one considered here is that of NOILC which is based on a quadratic (norm) optimal formulation [20] where, at each iteration, the following performance index is minimized to obtain the system input time series vector to be used for that iteration:

$$J_{k+1}(u_{k+1}) = \|e_{k+1}\|_Q^2 + \|u_{k+1} - u_k\|_R^2 \quad (8)$$

The minimization is subject to the dynamic constraint that $e_{k+1} = r - Gu_{k+1}$. Here, in general, Q and R are symmetric, positive definite weighting matrices, $\|e\|_Q^2$ denotes the quadratic form $e^T Q e$ and similarly with $\|\cdot\|_R^2$. Solving this optimization problem gives the following optimal choice for the time series vector u_{k+1}

$$u_{k+1} = u_k + G^* e_{k+1} \quad (9)$$

where G^* is the adjoint operator of G in the chosen Hilbert space topologies and can be expressed as

$$G^* = R^{-1}G^T Q. \quad (10)$$

Remark 5 *Note that the matrices R and Q only provide scaling of the input and output signals and hence, without loss of generality, in what follows they are chosen as $R =$*

$Q = I$ when G^ can be identified as $G^* = G^T$. With $R = Q = I$, the time series inner products reduce to $\langle f_1, f_2 \rangle = f_1^T f_2$ and the norms to Euclidean norms.*

In the original NOILC papers [11], [21] $Q = qI$ and $R = rI$ where $r > 0$ and $q > 0$ are scalars. This leads to an optimal control problem solved by Riccati methods. This is the case assumed in what follows.

This algorithm has many important properties [20]. In particular,

- (1) The change in input $u_{k+1} - u_k$ converges to zero in norm.
- (2) For discrete system, the input $\{u_k\}$ converges, and the limit is the input that produces the required output trajectory $y = r$ exactly. That is, the error norm converges to zero.
- (3) The error sequence has the important property that the error norm (mean square error value) decreases monotonically, i.e. $\|e_{k+1}\| < \|e_k\|, \forall k \geq 0$.
- (4) NOILC can be implemented using a feedforward (trial to trial) and current trial Riccati state feedback elements.

More details on NOILC can be found in [11], [21], [22], [23], [20].

2.3 Non-minimum phase plants in iterative learning control

In many cases, NOILC has shown its ability to achieve both rapid convergence and accurate tracking performance. There are however important exceptions illustrated by the following example.

Example 0 *The example has two parts, the first of which considers the system with minimum-phase transfer function*

$$G(s) = \frac{5(s+1)}{(s+2)(s+1/2)}, \quad (11)$$

and the second, non-minimum-phase system is as above but with $s+1$ replaced with $s-1$. In both cases the system is sampled using a zero-order hold with a sampling time of 0.1sec. The chosen trial length is 10s (from which $N = 100$) and the reference signal is a sampled version of the sine-wave $r(t) = \sin(\frac{4\pi}{3}t)$ shown in Figure 1. The initial input time series is chosen to be $u_0 = 0$ for simplicity.

The minimum-phase case has discrete transfer function

$$G(z) = \frac{0.4647(z - 0.9049)}{(z - 0.8187)(z - 0.9512)} \quad (12)$$

with a zero at $z = 0.9049$. The simulation was run over 20 iterations using the NOILC algorithm and the result is

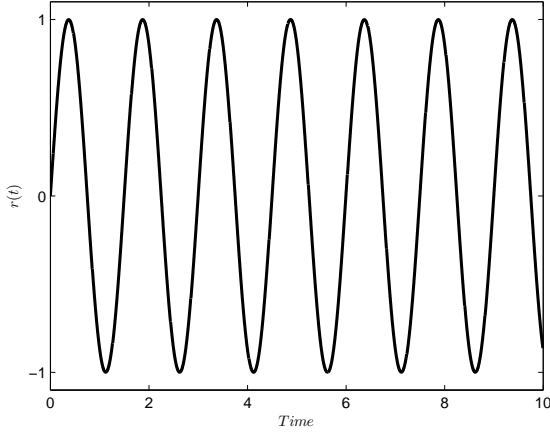


Fig. 1. The Reference Signal $r(t)$

shown in Figure 2 which indicates a reduction (improvement) in error norm by a factor of approximately 10^3 in 20 iterations and a factor of around 10^2 in six iterations. This indicates both high accuracy and rapid convergence.

Convergence can, however, be associated with poor performance when the plant is non-minimum phase. Error convergence to zero is still guaranteed but the convergence behavior is very different. Figure 3 shows error norm the convergence behavior for the transfer function above with the numerator polynomial replaced by $(s-1)$. In this case the discrete transfer function is

$$G(z) = \frac{0.4186(z - 1.1055)}{(z - 0.8187)(z - 0.9512)} \quad (13)$$

with a zero at $z = 1.1055$.

The algorithm is seen to reduce error norms rapidly in the first few trials but then it stagnates, moving along a "plateau" of almost constant error norm with only very small changes from iteration to iteration. For all practical purposes, (i) the input after the 6th trial barely changes and hence (ii) the error appears to be converging to a non-zero value. A significant problem is that the non-zero error achieved is, in this case, only a reduction of a factor of approximately 7.4 in norm over the initial error norm. In practical terms, this is an entirely unsatisfactory outcome. The task undertaken by this paper is to explain why this is happening and to model the behavior with the intention of predicting the stagnated values and signals that will be seen on the plateau.

Remark 6 Although it is intuitively clear from the examples and associated graphics what is meant by the "stagnated value" or "plateau", it ultimately has no asymptotic mathematical meaning for the NOILC algorithm. This is because the error is, in fact, simply converging to zero at an infinitesimally slow rate. The

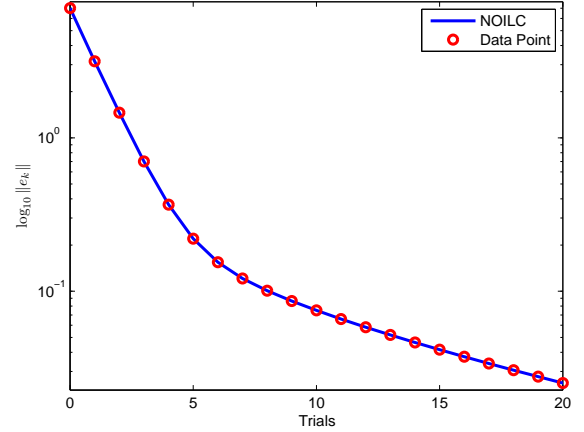


Fig. 2. Tracking error norm of NOILC for a typical minimum phase system

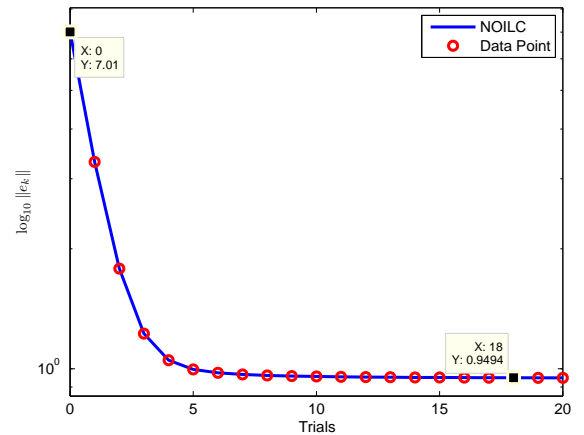


Fig. 3. Non-minimum phase example with apparent convergence to a non-zero, large error

plateau seen in the example is therefore a visual phenomenon valid for a large but finite number of iterations but, ultimately, has no relevance to final convergence to zero. Its meaning is therefore transient but valuable as it is what will be observed in practice and is what will ultimately limit the practical tracking accuracy achievable. In what follows, the plateau is taken to be a value typical of error norm values at the onset of slow convergence. This is quantified in terms of behaviours in subspaces.

In the following analysis, attention is focussed on the case of single-input single-output systems with m non-minimum phase zeros $\{z_j : |z_j| > 1, 1 \leq j \leq m\}$. It will be shown that the NOILC algorithm exhibits two different convergence rates characterized by factoring the space of all possible error functions into two subspaces. One of these is associated with the span of time series vectors generated typified by time series of the form $\{z_j^{-t}, t = 0, \dots, N - k^*\}, 1 \leq j \leq m$. This subspace will

be denoted by \mathcal{E}_+ and will be seen to be associated with the onset of slow convergence if the time interval $[0, N]$ is 'long'. The other subspace can be taken to be its orthogonal complement \mathcal{E}_+^\perp .

3 Characterization of \mathcal{E}_+

Suppose the non-minimum phase (NMP) system with transfer function $G(z)$ has m NMP zeros

$$G(z) = \frac{\prod_{i=1}^{i_0} (z - b_i) \prod_{i=1}^m (z - z_i)}{\prod_{i=1}^n (z - a_i)} \quad (14)$$

where $|z_i| > 1, i = 1, \dots, m$ are NMP zeros outside the unit circle.

Remark 7 *It is also assumed that $|b_j| < 1, 1 \leq j \leq i_0$. The rare case when a zero exists on the unit circle is technically more complex and is not considered in this paper.*

$G(z)$ can be decomposed into the product

$$G(z) = G_m(z)G_a(z), \quad (15)$$

where

$$G_m(z) = \frac{\prod_{i=1}^{i_0} (z - b_i) \prod_{i=1}^m (1 - z_i z)}{\prod_{i=1}^n (z - a_i)} \quad (16)$$

is minimum phase and

$$G_a(z) = \frac{\prod_{i=1}^m (z - z_i)}{\prod_{i=1}^m (1 - z_i z)} \quad (17)$$

is all-pass (i.e. $|G(z)| \equiv 1, \forall |z| = 1$). In matrix form, this can be written [17]

$$G = G_m G_a,$$

where G, G_m and G_a are the lifted matrix representations of $G(z), G_m(z), G_a(z)$, respectively.

Remark 8 *The matrices G_a and G_m operate on the associated time series vectors in a manner described by the transfer functions $G_a(z)$ and $z^{k^*} G_m(z)$ respectively as $G_a(z)$ (resp. $G_m(z)$) has relative degree zero (resp. k^*).*

The chosen time series subspace \mathcal{E}_+ will be seen to be defined by

$$\mathcal{E}_+ = (G_m^T)^{-1} \mathcal{E}_{a+}, \quad (18)$$

where \mathcal{E}_{a+} is defined in the next section.

3.1 Construction of \mathcal{E}_{a+}

Suppose that $G(z)$ has m NMP plane zeros described by the list $\{z_i : 1 \leq i \leq m_0\}$ with z_i having multiplicity n_i and $\sum_{i=1}^{m_0} n_i = m$. Using the notation

$$\gamma_0(z) = [1, z, z^2, \dots, z^{N-k^*}]^T,$$

define, for $1 \leq \ell \leq n_i, 1 \leq i \leq m_0$, the vectors

$$\gamma_{i\ell} = \frac{d^{\ell-1}}{dz^{\ell-1}} \gamma_0(z)|_{z=z_i} \quad (19)$$

For example, if z_1 has multiplicity $n_1 = 3$, it follows that

$$\gamma_{11} = [1, z_1, z_1^2, z_1^3, \dots, z_1^{N-k^*}]$$

$$\gamma_{12} = [0, 1, 2z_1, 3z_1^2, \dots, (N-k^*)z_1^{N-k^*-1}]$$

$$\gamma_{13} = [0, 0, 2, 6z_1, \dots, (N-k^*)(N-k^*-1)z_1^{N-k^*-2}]$$

Next reverse the order of the elements in $\gamma_{i\ell}$ to construct a vector $\alpha_{i\ell}$ as

$$\alpha_{i\ell} = [\gamma_{i\ell}(N-k^*) \ \gamma_{i\ell}(N-k^*-1) \ \dots \ \gamma_{i\ell}(1)]^T. \quad (20)$$

It is easy to show that $\alpha_{i\ell}, 1 \leq \ell \leq n_i, 1 \leq i \leq m_0$ are linear independent.

\mathcal{E}_{a+} is now defined by the relation

$$\mathcal{E}_{a+} = \text{span}\{\alpha_{i\ell}, 1 \leq \ell \leq n_i, 1 \leq i \leq m_0\}, \quad (21)$$

$$\dim(\mathcal{E}_{a+}) = m$$

Remark 9 *Noting that $\frac{1}{(1-z_i z^{-1})} = \gamma_0(z_i) \gamma_0(z^{-1}) + O((z_i/z)^{-(N+1-k^*)})$, a simple calculation indicates that, for each $1 \leq \ell \leq n_i, 1 \leq i \leq m_0$, the time series represented by $\gamma_{i\ell}$ is generated by the impulse response of the transfer function*

$$\frac{z^{-(\ell-1)}(\ell-1)!}{(1-z_i z^{-1})^\ell},$$

Remark 10 *In the generic case of $n_i = 1, \forall i$, a simple calculation shows that these vectors have the notationally simpler form, $i = 1, \dots, m$,*

$$\alpha_i = [z_i^{N-k^*} \ z_i^{N-k^*-1} \ \dots \ 1]^T = z_i^{N-k^*} \gamma_0(z_i^{-1})$$

the space of error time series \mathcal{E} can be divided into two parts: $\mathcal{E} = \mathcal{E}_+ \oplus \mathcal{E}_+^\perp$, where, if $|z_0^{-2N}|$ is small enough,

- (1) the change in error from iteration to iteration in the subspace \mathcal{E}_+ is small and hence the error norm of the projection onto this subspace decreases very slowly.
- (2) All substantial activity in error norm reduction can be regarded as taking place in the orthogonal subspace \mathcal{E}_+^\perp .
- (3) As the error norm is monotonically decreasing, the error norm will "plateau" out once the activity in \mathcal{E}_+^\perp is completed.

These observations, in the author's opinion, convincingly explain and parameterize what is happening in the case of NOILC applied to NMP systems. The analysis is not relevant to minimum phase systems as, in this case, it is natural to take $G_a(z) = 1$, $G_a = I$ and hence $\mathcal{E}_{a+} = \{0\}$.

Remark 16 *Note that the basis for the validity of above results is that $\delta^2(N) = O(|z_0^{-2N}|)$ is sufficiently small, which is clearly related to the positions of NMP zeros, as well as the time interval N . A simple interpretation of the condition that $|z_0^{-2N}|$ is small is that the underlying time interval $[0, N]$ is long relative to the "time constants" associated with the zeros of the system. This is consistent with the observations in [11].*

Finally, for the special, but important, case of $m = 1$, consider the following all pass system

$$G_a(z) = \frac{1 - z_1^{-1}z}{z - z_1^{-1}} = -z_1^{-1} + \sum_{j=1}^{\infty} b_j z^{-j}, \quad z_0 > 1 \quad (36)$$

Its matrix form is

$$G_a = \begin{bmatrix} -z_1^{-1} & & & & \\ b_1 & -z_1^{-1} & & & \\ \vdots & \ddots & \ddots & & \\ b_{N-1} & \cdots & b_1 & -z_1^{-1} & \end{bmatrix} = U \begin{bmatrix} \delta_1 & & & & \\ & 1 & & & \\ & & \ddots & & \\ & & & \ddots & \\ & & & & 1 \end{bmatrix} V^T$$

Taking determinants, gives the smallest singular value as $\underline{\sigma}(G_a) = \delta_1 = |z_1|^{-(N+1-k^*)}$. It follows that $\delta(N) = |z_1|^{-(N+1-k^*)}$ which provides a useful explicit relationship with the position of the zero z_1 and the time interval N .

4 Modelling Slow Convergence using Linear Constraints

The analysis and interpretation presented in the previous section is now used to motivate the construction of

an approximate mathematical model of the onset of slow convergence behaviour of NOILC for a non-minimum phase system G under the assumption that the time interval N is sufficiently long (or, more precisely, $|z_j^{-2N}|$ is sufficiently small for all $1 \leq j \leq m$). Details are given below.

4.1 Construction of an approximate model of slow convergence

To construct the approximate model, motivated by (35) it is assumed that, to a good approximation, and for the purposes of calculation, a good prediction of behavior over a large number of trials can be described by replacing $O(|z_0^{-2N}|)$ by zero (equivalent to setting $\delta_i = 0, 1 \leq i \leq m$). That is, the approximate model of NOILC performance up to the onset of slow convergence will assume that the error sequence satisfies the following linear constraint(s) for a large number of iterations:

$$\langle e_{k+1} - e_k, \beta \rangle = 0, \quad \forall \beta \in \mathcal{E}_+. \quad (37)$$

Equivalently,

$$\langle e_{k+1} - e_k, \beta_i \rangle = 0, \quad 1 \leq j \leq m \quad (38)$$

As $e_{k+1} - e_k = -G(u_{k+1} - u_k)$, this constraint can be written as $u_{k+1} \in \Omega_{k+1}$ where

$$\Omega_{k+1} = \{u : \langle u - u_k, \psi_j \rangle = 0, 1 \leq j \leq m\} \quad (39)$$

Here $\psi_j = G^T \beta_j, 1 \leq j \leq m$ span the subspace $G^T \mathcal{E}_+$.

Remark 17 *The introduction of these linear constraints is the mechanism used to construct the proposed model of algorithm evolution that explains and predicts the behavior of NOILC when applied to plants with NMP zeros. The implications of this are analyzed below. The approximation will break down as iterations progress as, ultimately, the error does go to zero. The model is proposed as a good approximation over initial and possibly large number of trials where onset of the plateau/stagnation effect is seen in practice.*

The model of NOILC behavior when applied to a non-minimum phase system is that

- (1) the signal u_{k+1} computed from NOILC can be approximated by the solution of the constrained optimization problem

$$u_{k+1} = \arg \min_{u_{k+1} \in \Omega_{k+1}} J_{k+1}(u_{k+1})$$

- (2) and that the limit, as $k \rightarrow \infty$, of these solutions provides a good approximation to behavior on the plateau.

4.2 Lagrange multiplier solution of the approximate model

The solution to the constrained optimization problem is approached using Lagrange multiplier techniques i.e. by minimizing the Lagrangian

$$J_{k+1}^\lambda = \frac{1}{2}J_{k+1} + \sum_{j=1}^m \lambda_j \langle \psi_j, u_{k+1} - u_k \rangle \quad (40)$$

over all $u_{k+1} \in \Omega_{k+1}$ and all scalars λ_j (the Lagrange multipliers). The necessary condition for a minimum is that J_{k+1}^λ is stationary at the optimal u_{k+1} and suitable values of $\lambda = [\lambda_1, \lambda_2, \dots, \lambda_m]^T$.

Remark 18 *The addition of these constraints will be seen to retain all properties of the NOILC algorithm except that the error sequence $\{e_k\}_k \geq 0$ does not necessarily converge to zero.*

The solution of this problem is stated in the following theorem which uses the definition of P_ϵ to denote the self-adjoint, orthogonal projection onto the span of m linearly independent vectors $\epsilon_1, \dots, \epsilon_m$. In more detail,

$$P_\epsilon = [\epsilon_1, \epsilon_2, \dots, \epsilon_m] M_\epsilon^{-1} \theta_\epsilon(x) \quad (41)$$

where M_ϵ is the symmetric, positive definite (and hence nonsingular) $m \times m$ matrix with (i, j) element $\langle \epsilon_i, \epsilon_j \rangle$ and $\theta_\epsilon(x)$ is the $m \times 1$ vector with i th element $\langle \epsilon_i, x \rangle$. P_ϵ has the properties:

$$P_\epsilon x = x \quad \forall x \in \text{span}\{\epsilon_j : 1 \leq j \leq m\} \quad (42)$$

$$P_\epsilon x = 0 \quad \forall x \in \text{span}\{\epsilon_j : 1 \leq j \leq m\}^\perp \quad (43)$$

$$\|P_\epsilon\| = 1 \quad (44)$$

$$(I - P_\epsilon) \geq 0 \quad (45)$$

Theorem 5 *Using the above notation and constructions, the solution of the constrained NOILC algorithm on the $(k+1)$ th iteration takes the form*

$$u_{k+1} - u_k = (I - P_\psi) G^T e_{k+1} \quad (46)$$

and the error evolution

$$e_{k+1} = L e_k, \quad L = (I + G(I - P_\psi) G^T)^{-1} e_k \quad (47)$$

The error norm has the monotonicity property

$$\|e_{k+1}\| \leq \|e_k\|, \quad \forall k \geq 0 \quad (48)$$

In addition, e_k converges to e_∞ (in the norm topology) and it can be computed from the formula $e_\infty = P_\beta e_0$, or, equivalently,

$$e_\infty = \sum_{j=1}^m \gamma_j \beta_j, \quad \gamma = [\gamma_1, \dots, \gamma_m]^T = M_\beta^{-1} \theta_\beta(e_0) \quad (49)$$

The limiting norm can be computed using

$$\|e_\infty\|^2 = \theta_\beta(e_0)^T M_\beta^{-1} \theta_\beta(e_0) \quad (50)$$

Proof. Firstly note that the choice $u = u_k$ is suboptimal and the monotonicity property is easily proved. The conditions for a stationary point of the Lagrangian consists of the constraint equations and, taking the Fréchet derivative with respect to u_{k+1} , the equality

$$u_{k+1} - u_k = G^T e_{k+1} - \sum_{j=1}^m \lambda_j \psi_j \quad (51)$$

Taking the inner product with ψ_i and using the constraints,

$$0 = \langle \psi_i, G^T e_{k+1} \rangle - \sum_{j=1}^m \lambda_j \langle \psi_i, \psi_j \rangle, \quad 1 \leq i \leq m \quad (52)$$

which is just $0 = \theta_\psi(G^T e_{k+1}) - M_\psi \lambda$. It follows that

$$u_{k+1} - u_k = G^T e_{k+1} - \sum_{j=1}^m \lambda_j \psi_j = (I - P_\psi) G^T e_{k+1} \quad (53)$$

Now operate with G to give

$$e_{k+1} - e_k = -G(I - P_\psi) G^T e_{k+1},$$

which can be written as

$$e_{k+1} = (I + G(I - P_\psi) G^T)^{-1} e_k = L e_k \quad (54)$$

with the natural identification of the Learning Operator L . This gives

$$e_k = (I + G(I - P_\psi) G^T)^{-k} e_0 = L^k e_0 \quad (55)$$

The following three important invariance properties are now demonstrated

$$L|_{\mathcal{E}_+} = I, \quad L\mathcal{E}_+^\perp \subset \mathcal{E}_+^\perp, \quad \|L|_{\mathcal{E}_+^\perp}\| < 1 \quad (56)$$

where $L|_S$ denotes the restriction of the linear operator L to the subspace S .

Consider the above error evolution equation and write

$$\begin{aligned} e_0 &= e_{0+} + e_{0+}^\perp, \\ e_{0+} &= P_\beta e_0 \in \mathcal{E}_+, \\ e_{0+}^\perp &= (I - P_\beta) e_0 \in \mathcal{E}_+^\perp \end{aligned} \quad (57)$$

By construction, $(I - P_\psi)G^T \mathcal{E}_+ = \{0\}$ so that

$$(I + G(I - P_\psi)G^T)e_{0+} = e_{0+}. \quad (58)$$

It immediately follows that the restriction $L|_{\mathcal{E}_+}$ of learning operator L to \mathcal{E}_+ is the identity i.e. $L|_{\mathcal{E}_+} = I$. In particular, $L^k e_{0+} = e_{0+}$ for all $k \geq 0$.

Now let $\tilde{v} \in \mathcal{E}_+^\perp$ be arbitrary and set $v = L\tilde{v}$ or, equivalently, $\tilde{v} = L^{-1}v$. Taking the inner product with arbitrary $w \in \mathcal{E}_+$ then gives

$$\begin{aligned} 0 &= \langle w, \tilde{v} \rangle \\ &= \langle w, (I + G(I - P_\psi)G^T)v \rangle \\ &= \langle (I + G(I - P_\psi)G^T)w, v \rangle \\ &= \langle w, v \rangle. \end{aligned} \quad (59)$$

It follows that $v \in \mathcal{E}_+^\perp$ and hence that $L\mathcal{E}_+^\perp \subset \mathcal{E}_+^\perp$.

Now examine the quadratic form $\langle x, L^{-1}x \rangle$ with $x \in \mathcal{E}_+^\perp$ arbitrary but non-zero. Note that $\langle x, G(I - P_\psi)G^T x \rangle \geq 0$, equality holding if, and only if, $(I - P_\psi)G^T x = 0$ i.e. $x \in \mathcal{E}_+$. As $\mathcal{E}_+ \cap \mathcal{E}_+^\perp = \{0\}$, it follows that $x = 0$ which is a contradiction. Hence there exists $\sigma^2 > 0$ such that

$$\langle x, L^{-1}x \rangle \geq (1 + \sigma^2)\|x\|^2. \quad (60)$$

It follows that $\|L|_{\mathcal{E}_+^\perp}\| \leq \frac{1}{1+\sigma^2} < 1$.

The error evolution equation can now be written as

$$\begin{aligned} e_k &= L^k e_0 = L^k e_{0+} + L^k e_{0+}^\perp \\ &= (L|_{\mathcal{E}_+})^k e_{0+} + (L|_{\mathcal{E}_+^\perp})^k e_{0+}^\perp \\ &= e_{0+} + (L|_{\mathcal{E}_+^\perp})^k e_{0+}^\perp \end{aligned} \quad (61)$$

from which, using $\|L|_{\mathcal{E}_+^\perp}\| < 1$ from the above, gives

$$\lim_{k \rightarrow \infty} e_k = e_{0+} = P_\beta e_0. \quad (62)$$

According to the definition of \mathcal{E}_+ , it immediately follows that $e_\infty = \sum_{j=1}^m \gamma_j \beta_j$ where $\gamma = [\gamma_1, \dots, \gamma_m]^T = M_\beta^{-1} \theta_\beta(e_0)$ and hence the error norm $\|e_\infty\|^2$ can be computed as required. This completes the proof of the theorem. \blacksquare

The theorem is a precise description of properties of the proposed constrained NOILC model. In what follows, these ideas are interpreted in terms of anticipated performance of the real NOILC algorithm.

Summary and Interpretation of the Results: Consider a single input single output, stable non-minimum

phase system with NMP zeros $z_j, 1 \leq j \leq m$, outside the unit circle satisfying the condition that all values of $|z_j^{-2N}|, 1 \leq j \leq m$ are sufficiently small. Then, convergence takes the form of initial reductions in error norm in \mathcal{E}_+^\perp followed by a 'plateau' where error norms in \mathcal{E}_+ reduce infinitesimally from iteration to iteration. The chosen model of the effect of these zeroes as linear equality constraints on the dynamics of NOILC characterizes predicts the error e_∞ on the 'plateau' as follows

$$e_\infty = \sum_{j=1}^m \gamma_j \beta_j, \quad \gamma = [\gamma_1, \dots, \gamma_m]^T = M_\beta^{-1} \theta_\beta(e_0) \quad (63)$$

and the value of error norm along the plateau using

$$\|e_\infty\|^2 = \theta_\beta(e_0)^T M_\beta^{-1} \theta_\beta(e_0). \quad (64)$$

The real (unconstrained) NOILC algorithm moves along this plateau for many iterations but ultimately drifts away from the plateau to converge to zero error. This can typically take more iterations than are practical for applications purposes and will not be observed.

Remark 19 In the case when the plant has only one NMP zero z_1 the equations simplify to produce

$$e_\infty = \frac{\beta_1^T e_0}{(\beta_1^T \beta_1)} \beta_1, \quad \|e_\infty\|^2 = \frac{(\beta_1^T e_0)^2}{(\beta_1^T \beta_1)} \quad (65)$$

where $\beta_1 = (G_m^T)^{-1} \alpha_1 = (G_m^T)^{-1} z_1^{N-k^*} \gamma_0(z_1^{-1})$.

This formula can be simplified using an approximation replacing β_1 by $\gamma_0(z_1^{-1})$ (increasingly valid as the $z_1^{-N} \rightarrow 0$) motivated by the asymptotic characterization

$$\lim_{N \rightarrow \infty} z_1^{-(N-k^*)} \beta_1 = z_1^{-k^*} G_m^{-1}(z_1) \gamma_0(z_1^{-1}) \quad (66)$$

and the fact that the formulae are unchanged if β_1 is scaled. This result is proved in an Appendix.

Using this approximation,

$$e_\infty \approx (\gamma_0(z_1^{-1})^T e_0) \frac{1 - z_1^{-2}}{(1 - z_1^{-2(N+1-k^*)})} \begin{bmatrix} 1 \\ z_1^{-1} \\ \vdots \\ z_1^{-(N-k^*)} \end{bmatrix} \quad (67)$$

and

$$\|e_\infty\|^2 \approx (\gamma_0(z_1^{-1})^T e_0)^2 \frac{(1 - z_1^{-2})^2}{(1 - z_1^{-2(N+1-k^*)})}, \quad (68)$$

The above can be used to complete this section. More precisely, it is noted that the error seen on the plateau

is small only when $\theta_\beta(e_0)$ is small. This can be achieved under two conditions only:

- (1) The initial tracking error signal e_0 is small in norm or, more generally,
- (2) the quantities $\langle \beta_j, e_0 \rangle, 1 \leq j \leq m$ are all small, which can be true if e_0 is not small but is small in some time interval $[0, N_0] \subset [0, N]$ with $|z_j^{N_0}| \gg 1, 1 \leq j \leq m$. This could be achieved naturally if, for example, the plant has zero initial conditions and the reference r is zero in $[0, N_0]$. Choosing $u_0(t)$ to be zero in this interval achieves the objective with no effort.

5 Numerical Simulation

In this section, numerical examples are provided to verify the analysis results. The simulation compare the prediction with real simulation using different time intervals, as well as different initial choices.

Consider the following non-minimum phase system

$$G(s) = \frac{5(s-1)}{(s+2)(s+1/2)}, \quad (69)$$

which is sampled using zero-order hold and a sampling time of 0.1s. The consequent discrete time model is

$$G(z) = \frac{0.4186(z-1.1055)}{(z-0.8187)(z-0.9512)}$$

and there is a single NMP discrete zero at $z_1 = 1.1055$ (so that $z_0 = z_1$).

Example 1 *The trial length is set to the relatively small value of $T = 3$ (only 50% more than the slowest time constant and only three times the time constant associated with the NMP zero). The number of sample intervals $N = T/\text{step} = 30$ and the reference is a sampled version of the sine-wave $\sin(\frac{4\pi}{3}t)$ shown in Figure 4. The initial input is chosen to be $u_0(t) = 0, t = 0, \dots, N-1$. The simulation was run over 20 iterations which is sufficient to demonstrate the main performance characteristics.*

In this case, the critical value $\delta^2(N) = z_0^{-2N} = 0.0024$. The simulation results are shown in Figure 5 and Figure 6, where slow convergence is not observed as there are substantial differences between the approximate model predictions and the simulation results over this iteration range. The algorithm does however provide a good indication of where convergence begins to slow (between iterations 3 and 5) but the plateau effect is not strong in this case. This is explained intuitively by the observation that the trial length $T = 3$ is not large compared with the 'time constant' $T_z = 1$ associated with the zero. The next example increases T to verify this.

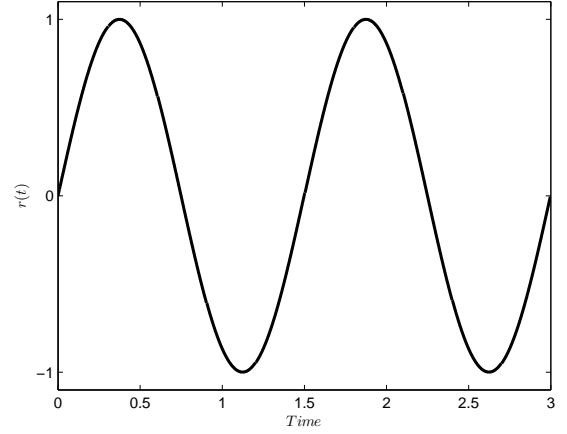


Fig. 4. The Reference Signal $r(t)$

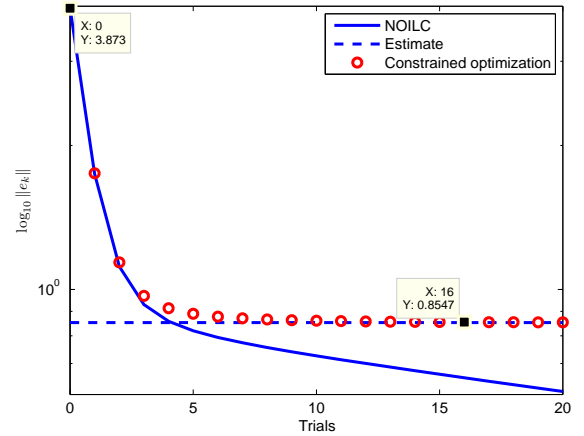


Fig. 5. Comparison of Convergence for $T = 3s$

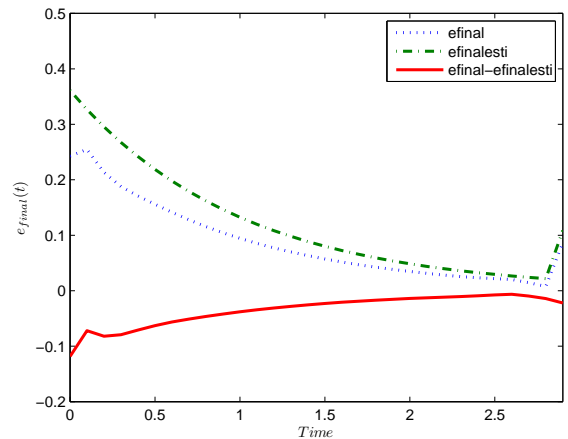


Fig. 6. Comparison of the Final Tracking Error $e_{20}(t)$ with its estimate

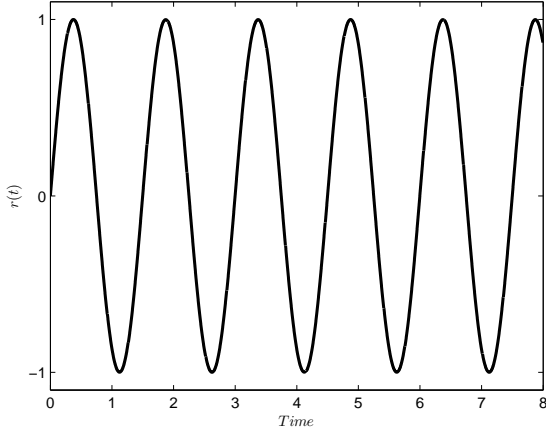


Fig. 7. The Reference Signal $r(t)$

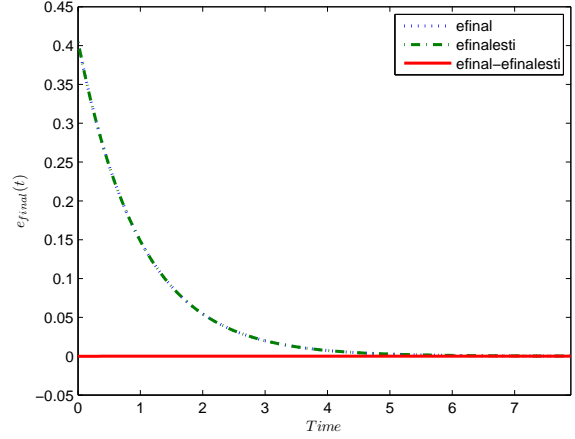


Fig. 9. Comparison of the Final Tracking Error $e_{40}(t)$ with its estimate

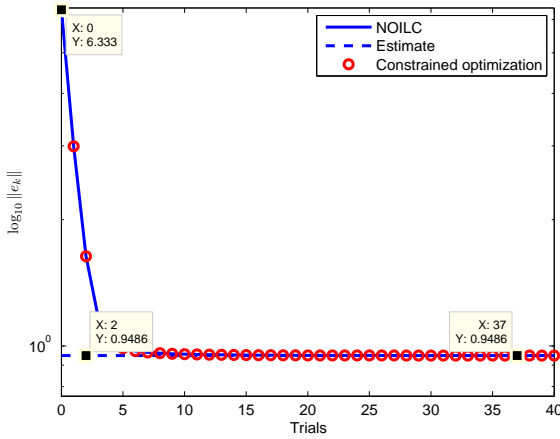


Fig. 8. Comparison of Convergence

Example 2 The trial length is now increased to the value $T = 8$ and the reference signal is the sine-wave input $r(t) = \sin(\frac{4\pi}{3}t)$ shown in Figure 7. The initial input is chosen to be $u_0(t) = 0, t = 0, \dots, N - 1$. The simulation was now run over 40 iterations and the results are shown in Figure 8 and Figure 9.

It can be seen the approximated model proposed now provides a good, accurate description of the slow convergence phenomenon over the iteration range displayed, the plateau is well defined visually and this 'final' tracking error on the plateau is estimated to a high accuracy.

Finally, the proposed model predicts that the plateau value $\|e_\infty\|^2$ depends on the initial error e_0 and hence the initial control input u_0 . To verify this and also to show again that the results can predict observed behaviour accurately for different initial inputs, the inputs $u_0(t) = 0, u_0(t) = 100, u_0(t) = t$, were considered. The results are shown in Figure 10 again confirming the validity of the analysis results.

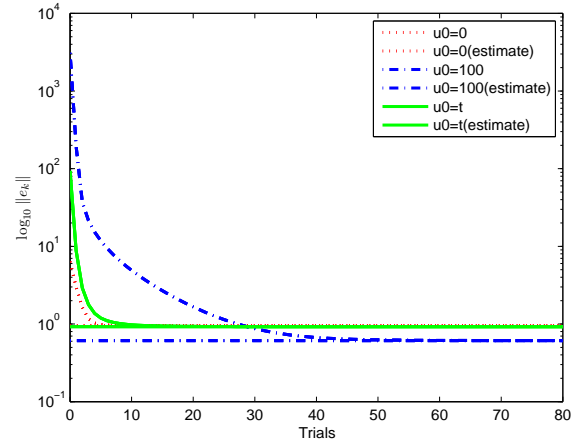


Fig. 10. Comparison of Convergence for $T = 8s$

The above examples show that the theory is capable of accurately predicting the effect of NMP zeros on tracking accuracy when that effect is substantial. The next example shows that this remains true even when the effect is small.

Example 3 The trial length is again $T = 8$ and the reference signal is generated by the sine-wave input $u^*(t) = \sin(\frac{4\pi}{3}t)$ shown in Figure 7. The initial input is chosen to be $u_0(t) = 0, t = 0, \dots, N - 1$. The simulation was run over 150 iterations and the results are shown in Figure 11 and Figure 12.

In this example, the optimal input u^* doesn't contain any exponentially increasing components and hence the effect of NMP zero was intuitively expected to be small but non-zero. From the figure, this is seen to be the case. It can be seen that even, in this case, the approximated model proposed provides a quite accurate description of the slow convergence phenomenon. The convergence per-

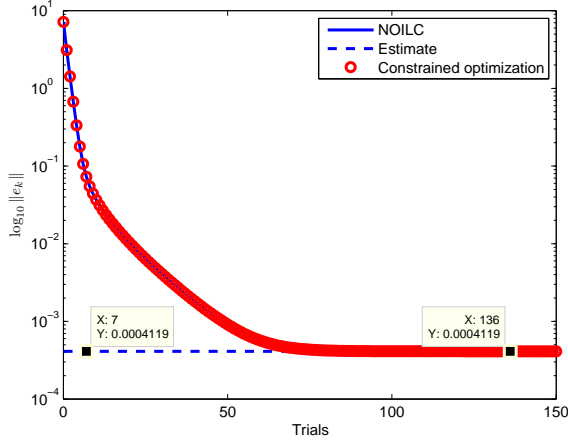


Fig. 11. Comparison of Convergence

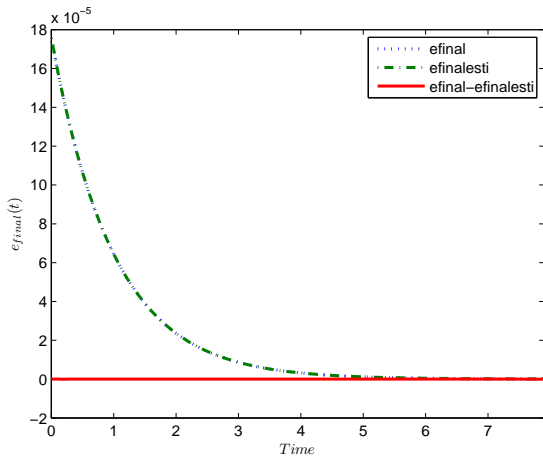


Fig. 12. Comparison of the Final Tracking Error $e_{200}(t)$ with its estimate

formance is well predicted and the 'final' tracking error on the plateau is estimated to a high accuracy.

Finally, different initial inputs are used to verified the results of the analysis. Figure 13 again confirms the validity of the analysis results.

6 Conclusion

The paper has modelled observed behavior of norm optimal iterative learning control (NOILC) when the plant has a number of non-minimum phase (NMP) zeros. This observed behavior consists of two phases of convergence. The first occurs in the first few iterations where the algorithm normally exhibits good (and potentially rapid) error norm reductions. The second phase then sets in and exhibits extremely slow reductions, typically so slow that, to all practical intents and purposes, the algorithm is not converging. The plot of error norm $\|e_k\|$ against

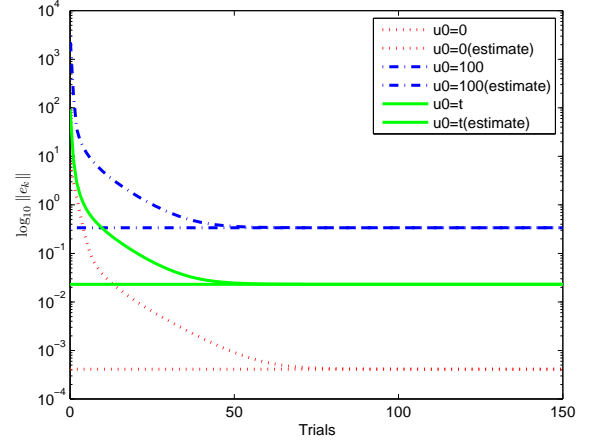


Fig. 13. Comparison of Convergence for $T = 8s$

k appears to form a plateau at a constant value that represents the best experimental accuracy that can be achieved in practice.

Based on the belief that it is important that this phenomenon and its implications for design are understood, the analysis has been used to motivate the construction of a model of the phenomenon. This was initiated by writing the plant as a product $G = G_m G_a$ where G_a is an all-pass network arising from the NMP zeros and G_m is minimum-phase. It was then proved that the self-adjoint operator $G_a G_a^T$ almost annihilates well-defined signals associated with the zeros. The span of these signals is an m -dimensional subspace \mathcal{E}_{a+} of the output signal space. It has then been proved that convergence of error projections into $\mathcal{E}_+ = (G_m^T)^{-1} \mathcal{E}_{a+}$ is inevitably slow whilst, in contrast, convergence of the component in the orthogonal complement \mathcal{E}_+^\perp can be rapid.

Based on this analysis, it has been proposed that, to a good approximation, the NOILC algorithm is behaving as if it is subject to m equality constraints (orthogonality conditions). These constraints are identified and the model has been used to predict both the values of the tracking error and error norm value associated with the plateau using Lagrangian methods. The model provides some insight into the effects of initial error e_0 and reference signal on the algorithm behavior and suggests that a small initial error and/or a reference signal with an initial period of inactivity are simple practical ways of improving performance and accuracy. Finally the predictions of the model have been shown to be good in various numerical simulations.

Further work is needed to generalize the ideas to the case of multi-input multi-output systems (where the same phenomenon occurs but the characterization of zeros is much more complex).

Finally, the formulae in this paper have been given for

the case of weightings $Q = R = I$. The relevant formulae for the more general case of $Q = qI, R = rI$ (where $q > 0, r > 0$ are scalars) are obtained by replacing the matrix representation G by $q^{1/2}Gr^{-1/2}$.

References

- [1] S. Arimoto, S. Kawamura, and F. Miyazaki. Convergence, stability and robustness of learning control schemes for robot manipulators. In M. J. Jamshidi, L. Y. Luh, and M. Shahinpoor, editors, *Recent Trends in Robotics: Modelling, Control, and Education*, pages 30–316. Elsevier, NY, USA, 1985.
- [2] P. Jiang, P. Y. Woo, and R. Unbehauen. Iterative learning control for manipulator trajectory tracking without any control singularity. *Robotica*, 20(2):149–58, 2002.
- [3] Y.Q. Wang, J. Shi, D.H. Zhou, and et al. Iterative learning fault-tolerant control for batch processes. *Industrial and Engineering Chemistry Research*, 45(26):9050–9060, 2006.
- [4] J.H. Lee and K.S. Lee. Iterative learning control applied to batch processes: An overview. *Control Engineering Practice*, 15(10):1306–1318, 2007.
- [5] H. Dou, K.K. Tan, T.H. Lee, and Z. Zhou. Iterative learning feedback control of human limbs via functional electrical stimulation. *Control Engineering Practice*, 7(3):315–325, 1999.
- [6] Y. C. Huang, M. Chan, Y. P. Hsin, and C. C. Ko. Use of PID and iterative learning controls on improving introral hydraulic loading system of dental implants. *JSME Int. J. Series C-Mechanical Systems Machine Elements and Manufacturing*, 46(4):144–1455, 2003.
- [7] S. Arimoto, S. Kawamura, and F. Miyazaki. Bettering operation of robots by learning. *Journal of Robotic Systems*, 1(2):123–140, 1984.
- [8] D.A. Bristow, M. Tharayil, and A.G. Alleyne. A survey of iterative learning control: A learning-based method for high-performance tracking control. *IEEE Control Systems Magazine*, 26(3):96–114, 2006.
- [9] H.-S. Ahn, K.L. Moore, and Y. Chen. Stability analysis of discrete-time iterative learning control systems with interval uncertainty. *Automatica*, 43(5):892–902, 2007.
- [10] D.H. Owens and J. Hatonen. Iterative learning control - an optimization paradigm. *Annual Reviews in Control*, 29(1):57–70, 2005.
- [11] N. Amann and D. H. Owens. Non-minimum phase plants in norm-optimal iterative learning control. Report, University of Exeter, 1994.
- [12] S. Gunnarsson and M. Norrlof. On the design of ILC algorithms using optimization. *Automatica*, 37(12):2011–2016, 2001.
- [13] X. Wang and D. Chen. An inversion-based iterative learning control algorithm for a class of nonminimum-phase systems. *IEE Proceedings: Control Theory and Applications*, 152(1):72–78, 2005.
- [14] C.T. Freeman, P.L. Lewin, and E. Rogers. Experimental evaluation of iterative learning control algorithms for non-minimum phase plants. *International Journal of Control*, 78(11):826–846, 2005.
- [15] J. Hatonen. *Issues of algebra and optimality in iterative learning control*. PhD thesis, University of Oulu, Finland, 2004.
- [16] J. Hatonen, D.H. Owens, and K.L. Moore. An algebraic approach to iterative learning control. *International Journal of Control*, 77(1):45–54, 2004.
- [17] D. H. Owens, J.J. Hatonen, and S. Daley. Robust monotone gradient-based discrete-time iterative learning control. *International Journal of Robust and Nonlinear Control*, 19(6):634–661, 2009.
- [18] Z. Bien and K.M. Huh. Higher-order iterative learning control algorithm. *IEE Proceedings, Part D: Control Theory and Applications*, 136(3):105–112, 1989.
- [19] J. Hatonen, D.H. Owens, and K. Feng. Basis functions and parameter optimisation in high-order iterative learning control. *Automatica*, 42(2):287–294, 2006.
- [20] N. Amann, D.H. Owens, and E. Rogers. Iterative learning control using optimal feedback and feedforward actions. *International Journal of Control*, 65(2):277–293, 1996.
- [21] N. Amann, D.H. Owens, and E. Rogers. Predictive optimal iterative learning control. *International Journal of Control*, 69(2):203–226, 1998.
- [22] N. Amann. *Optimal algorithms for iterative learning control*. PhD thesis, University of Exeter, UK, 1996.
- [23] N. Amann, D.H. Owens, and E. Rogers. Iterative learning control for discrete-time systems with exponential rate of convergence. *IEE Proceedings: Control Theory and Applications*, 143(2):217–224, 1996.
- [24] Ulf Grenander and Gabor Szego. *Toeplitz forms and their applications*. New York : Chelsea Publishing Company, second edition, 1984.

A Proof of Theorem 1

Proof. For any time series vector $u = [u(1), u(2), \dots, u(N-k^*)]^T \in R^{N+1-k^*}$, define

$$u(z) = \sum_{i=0}^{N-k^*} u(i)z^{-i}.$$

Using Parseval's theorem with $|G_a(z)| = 1, \forall |z| = 1$, yields

$$\begin{aligned} u^T G_a^T G_a u &\leq \frac{1}{2\pi i} \oint_{|z|=1} |G_a(z)u(z)|^2 \frac{dz}{z} \\ &= \frac{1}{2\pi i} \oint_{|z|=1} |u(z)|^2 \frac{dz}{z} = u^T u, \end{aligned} \quad (\text{A.1})$$

which implies

$$I - G_a^T G_a \geq 0, \quad \forall N \geq k^*. \quad (\text{A.2})$$

Hence, all the eigenvalues of $G_a^T G_a$ are less than or equal to one i.e. all singular values of G_a are less than or equal to one.

Consider the following equation

$$u^T (I - G_a^T G_a) u = 0. \quad (\text{A.3})$$

All non-zero solutions u are eigenvectors of $G_a^T G_a$ corresponding to eigenvalues equal to one, and they span a subspace of R^{N+1-k^*} whose dimension is identical to the number of singular values that are equal to one.

From (A.1), it can be seen that (A.3) holds if and only if the time series response $G_a(z)u(z)$ is zero for $t \geq N+1-k^*$. It is necessary to consider the following two cases.

Case 1: $N+1-k^* > m$. Consider the choice $u_0(z) = a_0 + a_1 z^{-1} + \dots + a_m z^{-m}$, then

$$G_a(z)u_0(z) = a_m + a_{m-1}z^{-1} + \dots + a_0 z^{-m}. \quad (\text{A.4})$$

It can be seen that the response $G_a(z)u_0(z)$ is zero for all $t > m$ and hence for all $t \geq N+1-k^*$. Therefore the equality in (A.1) holds. Hence $u_0 = [a_0 \ a_1 \ \dots \ a_m \ 0 \ \dots \ 0]^T$ is a solution of (A.3). Similarly, it can be found that the choices of

$$\begin{aligned} u_i(z) &= z^{-(i-1)}u_0(z) \\ &= a_0 z^{-(i-1)} + a_1 z^{-i} + \dots + a_m z^{-(m+i-1)} \end{aligned} \quad (\text{A.5})$$

where $i = 2, \dots, N+1-k^*-m$, also satisfy the equality in (A.1) and the corresponding vector time series $\{u_i\}$ are also solutions of (A.3). This provides $N+1-k^*-m$ linear independent solutions of (A.3).

Next, it is shown that there are no other solutions independent of $u_i, i = 1, 2, \dots, N+1-k^*-m$. This is proved by contradiction. Suppose there exists such a non-zero solution with transform $x(z) = \sum_{i=0}^{N-k^*} x(i)z^{-i}$, then there must exist a non-zero solution $x_0(z) = \sum_{i=N+1-k^*-m}^{N-k^*} x_0(i)z^{-i}$ (obtained by subtracting linear combinations of $u_i(z), i = 1, 2, \dots, N+1-k^*-m$ from $x_0(z)$). This, as will be seen, is impossible. To prove this notice that

$$\begin{aligned} G_a(z)x_0(z) &= \frac{a_0 + a_1 z + \dots + a_m z^m}{a_m + a_{m-1} + \dots + a_0 z^m} \\ &\times \sum_{i=N+1-k^*-m}^{N-k^*} x_0(i)z^{-i} \end{aligned} \quad (\text{A.6})$$

is finite length if and only if $x_0(z)$ cancels all the poles of $G_a(z)$. This, however, cannot happen because $x_0(z)$ has $m-1$ non-zero zeros while $G_a(z)$ has m non-zero poles.

It follows that there are exactly $N+1-k^*-m$ linear independent solutions of (A.3) and these correspond to $N+1-k^*-m$ singular values equal to one, which means $\sigma_i^{(N+1-k^*)} < 1$ for $1 \leq i \leq m$ and $\sigma_i^{(N+1-k^*)} = 1$ for $m+1 \leq i \leq N+1-k^*$.

Case 2: $N+1-k^* \leq m$ In this case, it can be seen from the discussion above that no solutions exist that satisfy

(A.3). Hence all the singular values must be less than one.

The proof is now complete. \blacksquare

B Proof of Theorem 2

Before proving Theorem 2, the following lemma is proved.

Lemma 1 For the given all pass system G_a , when $N+1-k^* > m$, the eigenspace of $G_a^T G_a$ has the following structure:

(i) the following $N+1-k^*-m$ linearly independent vectors are eigenvectors of $G_a^T G_a$ corresponding to the $N+1-k^*-m$ eigenvalues of 1:

$$\begin{aligned} v_1 &= [a_0 \ a_1 \ \dots \ a_m \ 0 \ \dots \ 0]^T \\ v_2 &= [0 \ a_0 \ a_1 \ \dots \ a_m \ \dots \ 0]^T \\ &\vdots \\ v_{N+1-k^*-m} &= [0 \ \dots \ 0 \ a_0 \ a_1 \ \dots \ a_m]^T \end{aligned}$$

each of which can be identified with time series with Z -transforms

$$\begin{aligned} v_i(z) &= z^{-(i-1)}(a_0 + a_1 z^{-1} + \dots + a_{m-1} z^{-(m-1)} \\ &\quad + a_m z^{-m}), i = 1, \dots, N+1-k^*-m \end{aligned}$$

(ii) The m eigenvectors of $G_a^T G_a$ corresponding to the m eigenvalues that are less than one form an m -dimensional subspace S_a .

(iii) If the zeros $\{z_i\}$ are distinct, then S_a is spanned by

$$\gamma_i = [1 \ z_i \ \dots \ z_i^{N-k^*}]^T, i = 1, \dots, m$$

each of which can be identified with the first $N+1-k^*$ terms of the impulse response of the transfer functions

$$\gamma_i(z) = \frac{1}{1 - z_i z^{-1}}, i = 1, \dots, m.$$

(iv) If one or more zeros has multiplicity $n_i > 1$, S_a is spanned by vectors, $1 \leq \ell \leq n_i, 1 \leq i \leq m_0$, computed from the vectors

$$\gamma_{i\ell} = \frac{d^{\ell-1}}{dz^{\ell-1}} \gamma_0(z)|_{z=z_i},$$

where $\gamma_0(z) = [1, z, z^2, \dots, z^{N-k^*}]^T$. Equivalently these vectors have elements equal to the first $N+1-k^*$ elements of the impulse response of

$$\frac{z^{-(\ell-1)}(\ell-1)!}{(1-z_iz^{-1})^\ell}, \quad 1 \leq \ell \leq n_i, 1 \leq i \leq m_0.$$

Proof. The first part (i) of this theorem follows directly from the proof of Theorem 1. Denote the subspace spanned by $v_i, i = 1, 2, \dots, N+1-k^*-m$ as V . Part (ii) follows from matrix algebra.

To prove parts (iii) and (iv), note that the eigenvectors of $G_a^T G_a$ corresponding to the m eigenvalues that are less than one span a subspace orthogonal to V , which is denoted as V^\perp .

Examining part (iii), note first that, as the z_i are distinct, the vectors $\gamma_i, i = 1, \dots, m$ are linearly independent (as they then form the columns in a nonsingular Van der Monde matrix). It only remains to prove that $\gamma_i \perp V, 1 \leq i \leq m$, when it follows that they span the subspace V^\perp of interest. This follows as

$$v_j^T \gamma_i = z_i^{j-1}(a_0 + a_1 z_i + a_2 z_i^2 + \dots + a_m z_i^m) = 0$$

from the definition of z_i .

The proof of (iv) requires more effort. For notational convenience, let $n(z) = a_0 + a_1 z + a_2 z^2 + \dots + a_m z^m$ from which it can be deduced that, for all $j \geq 1$,

$$\frac{d^{\ell-1}}{dz^{\ell-1}} [z^{j-1} n(z)] |_{z=z_i} = 0, \quad 1 \leq \ell \leq n_i, \quad 1 \leq i \leq m_0$$

Now define, $1 \leq \ell \leq n_i, 1 \leq i \leq m_0$,

$$\gamma_{i\ell} = \frac{d^{\ell-1}}{dz^{\ell-1}} \gamma_0(z) |_{z=z_i}, \quad \gamma_0(z) = [1, z, z^2, \dots, z^{N-k^*}]^T$$

A simple calculation then yields the orthogonality conditions, for all $j, 1 \leq \ell \leq n_i$ and $1 \leq i \leq m_0$

$$v_j^T \gamma_{i\ell} = \frac{d^{\ell-1}}{dz^{\ell-1}} [v_j^T \gamma_0(z)] |_{z=z_i} = 0$$

as

$$\frac{d^{\ell-1}}{dz^{\ell-1}} [v_j^T \gamma_0(z)] |_{z=z_i} = \frac{d^{\ell-1}}{dz^{\ell-1}} [z^{j-1} n(z)] |_{z=z_i} = 0.$$

It remains to relate these vectors to the transfer functions stated. To do this, note initially that the result follows trivially for $\ell = 1$ as γ_{i1} has elements that are equal to the coefficients in the power series expansion of

$$\frac{1}{1-z_iz^{-1}} = 1 + z_iz^{-1} + z_i^2 z^{-2} + z_i^3 z^{-3} + \dots$$

For $\ell > 1$, note that

$$\gamma_{i\ell} = \frac{d^{\ell-1}}{dz^{\ell-1}} \gamma_0(z) |_{z=z_i} = \frac{d^{\ell-1}}{dz_i^{\ell-1}} \gamma_0(z_i)$$

has elements that are the coefficients of $1, z^{-1}, z^{-2}, z^{-3}, \dots$ in the power series expansion of

$$\frac{\partial^{\ell-1}}{\partial z_i^{\ell-1}} \left[\frac{1}{1-z_iz^{-1}} \right] = \frac{z^{-(\ell-1)}(\ell-1)!}{(1-z_iz^{-1})^\ell}$$

That completes the proof of the lemma. ■

Moving on to the proof of Theorem 2.

Proof. Denote

$$F = \begin{bmatrix} 0 & \dots & \dots & 0 & 1 \\ 0 & \dots & \dots & 1 & 0 \\ 0 & \dots & 1 & 0 & 0 \\ \vdots & \vdots & \vdots & \ddots & \vdots \\ 1 & 0 & \dots & \dots & 0 \end{bmatrix} = F^T, \quad F^2 = I \quad (\text{B.1})$$

as the Euclidean norm preserving "time reversal matrix" (the matrix that reverses the order of elements in a time series vector), then [17] $G_a^T = F G_a F$. It follows that, if v is an eigenvector of $G_a^T G_a$ corresponding to eigenvalue λ , i.e. $G_a^T G_a v = \lambda v$, then $G_a G_a^T$ has an eigenvector Fv corresponding the eigenvalue λ . This statement follows from the identity

$$G_a G_a^T Fv = F F G_a F F G_a^T Fv = F G_a^T G_a v = F \lambda v = \lambda Fv. \quad (\text{B.2})$$

The proof is completed by defining $u_i = Fv_{N+2-k^*-i}$ as the eigenvectors with eigenvalue unity and setting $\alpha_{i\ell} = F\gamma_{i\ell}$ as the basis for the orthogonal invariant subspace spanned by eigenvectors with eigenvalues less than unity. ■

C Proof of Theorem 3

This section uses the notation of previous sections.

Proof. Consider the case when all zeros are distinct so that

$$\gamma_i = \gamma_0(z_i), \quad \& \quad \alpha_i = F\gamma_i = z_i^{N-k^*} \gamma_0(z_i^{-1}) \quad (\text{C.1})$$

According to the Courant-Fischer theorem,

$$\max(\delta_1, \dots, \delta_m) \leq \frac{\|G_a^T x\|}{\|x\|}, \quad (\text{C.2})$$

where $x \in \text{span}\{\alpha_i\}$. Write x as $x = \sum_{i=1}^m c_i \alpha_i$ from which

$$\begin{aligned} \|G_a^T x\| &= \|FG_a Fx\| = \|G_a Fx\| = \left\| \sum_{i=1}^m c_i G_a F \alpha_i \right\| \\ &= \left\| \sum_{i=1}^m c_i G_a \gamma_i \right\| \leq M \|c\|, \end{aligned} \quad (\text{C.3})$$

for some $M > 0$ with $c = [c_1, \dots, c_m]^T$. Moreover M can be chosen to be independent of N as, from the definitions, each $G_a \gamma_i$ is uniformly bounded in norm over N as its elements are the first $N + 1 - k^*$ elements of the impulse response of $G_a(z) \frac{1}{1-z_i z^{-1}}$ which is stable by construction.

Consider now the situation where $\|x\| = 1$ i.e. for some $\Gamma > 0$

$$\begin{aligned} 1 = \|x\| &= \|[\alpha_1, \dots, \alpha_m]c\| \\ &= \|[\gamma_0(z_1^{-1}), \dots, \gamma_0(z_m^{-1})]c\| \\ &\geq \Gamma \|\tilde{c}\| \\ &\geq \Gamma |z_0|^{N-k^*} \|c\| \end{aligned} \quad (\text{C.4})$$

where $\tilde{c} = \text{diag}\{z_i^{N-k^*}\}c$. Moreover, Γ can be chosen to be independent of N as the Hermitian matrix

$$[\gamma_0(z_1^{-1}), \dots, \gamma_0(z_m^{-1})]^* [\gamma_0(z_1^{-1}), \dots, \gamma_0(z_m^{-1})]$$

is nonsingular and monotonically increasing with $N + 1 - k^* \geq m$. Under these conditions,

$$\|c\| \leq \Gamma^{-1} |z_0|^{-(N-k^*)} \quad (\text{C.5})$$

so that

$$\|G_a^T x\| \leq M \|c\| \leq M \Gamma^{-1} |z_0|^{-(N-k^*)} = O(|z_0|^{-N}) \quad (\text{C.6})$$

This completes the proof. \blacksquare

D Characterization of the Behaviour of β_1 as $N \rightarrow \infty$

Note: The following calculations relate to the case where there are only distinct NMP zeroes i.e. $m_0 = m$ and all $n_i = 1$. For notational simplicity, only β_1 is considered but similar calculations can be used for any β_i .

Using the properties of the time reversal matrix F ,

$$\begin{aligned} \beta_1 &= (G_m^T)^{-1} \alpha_1 = (G_m^{-1})^T \alpha_1 \\ &= F G_m^{-1} F \alpha_1 = F G_m^{-1} \gamma_0(z_1) \end{aligned} \quad (\text{D.1})$$

Note that $G_m(z)$ is minimum phase and hence $G_m^{-1}(z)$ is asymptotically stable. Also $G_m^{-1} \gamma_0(z_1)$ can be identified with the first $N + 1 - k^*$ terms in the impulse response of $z^{-k^*} G_m^{-1}(z) \frac{1}{(1-z_1 z^{-1})}$ and hence, using partial fraction expansion, takes the form

$$G_m^{-1} \gamma_0(z_1) = \tilde{y} + z_1^{-k^*} G_m^{-1}(z_1) \gamma_0(z_1)$$

where \tilde{y} is the stable part of the response and is uniformly bounded in norm over N . It follows that

$$\begin{aligned} \beta_1 &= F G_m^{-1} \gamma_0(z_1) = F \tilde{y} + z_1^{-k^*} G_m^{-1}(z_1) F \gamma_0(z_1) \\ &= F \tilde{y} + z_1^{-k^*} G_m^{-1}(z_1) z_1^{N-k^*} \gamma_0(z_1^{-1}) \end{aligned}$$

and hence

$$\lim_{N \rightarrow \infty} z_1^{-(N-k^*)} \beta_1 = z_1^{-k^*} G_m^{-1}(z_1) \gamma_0(z_1^{-1}) \quad (\text{D.2})$$

That is, in any formula where scaling of β_1 does not affect the computations, β_1 can be replaced by $\gamma_0(z_1^{-1})$ with good accuracy if N is large.